Proceedings 1990 Conference
on Advanced Earth-to-Orbit Propulsion Technology
NASA, Huntsville, Alabama

ROTORDYNAMIC FORCES GENERATED BY DISCHARGE-TO-SUCTION LEAKAGE FLOWS IN CENTRIFUGAL PUMPS

A. Guinzburg, C. E. Brennen, A. J. Acosta and T. K. Caughey
California Institute of Technology
Division of Engineering and Applied Science
Pasadena, California 91125

ABSTRACT

This paper reviews the current state of knowledge of rotordynamic forces caused by the discharge-to-suction leakage flows in centrifugal pumps. The indications that these flows could contribute significantly to the rotordynamics motivated the fabrication of an experiment in which measurements of rotordynamic forces would be made on simulated leakage flows in which the flow rate, clearance, eccentricity and other parameters would be exercised in order to understand the phenomena. Sample data is presented and demonstrates substantial rotordynamic effects which could be potentially destabilizing. The rotordynamic forces appear to be inversely proportional to the clearance and change significant with the flow rate.

1. INTRODUCTION

In turbomachinery, the trend toward higher speeds and higher power densities has led to an increase in the number and variety of fluid-structure interaction problems in pumps, compressors, turbines and other machines. Fundamentally this occurs because the typical fluid forces scale like the square of the speed and thus become increasingly important relative to the structural strength. This becomes particularly acute in rocket engine turbopumps where demands to minimize the turbopump mass may also lead to reductions in the structural strength. This paper focuses on just one such fluid-structure interaction issue, namely the role played by fluid forces in determining the rotordynamic stability and characteristics of a turbopump. More specifically we review the contributions to the rotordynamic forces from the fluid flow through centrifugal pump impellers and the discharge-to-suction leakage flows external to the impeller. Results from an experimental program designed to measure these leakage flow contributions are described and analyzed.

2. BACKGROUND

Rotordynamic forces imposed on a centrifugal pump by the fluid flow through it were first measured by Domm and Hergt (1970), Hergt and Krieger (1969-70), Chamieh et al (1985) and Jery et al (1985). These forces are defined by expressing the instantaneous radial forces, $F_x^*(t)$ and $F_y^*(t)$ (figure 1) acting on the impeller in the linear form

$$\begin{bmatrix} F_x^*(t) \\ F_y^*(t) \end{bmatrix} = \begin{bmatrix} F_{OX}^* \\ F_{OY}^* \end{bmatrix} + [A] \begin{bmatrix} x(t) \\ y(t) \end{bmatrix} \tag{1}$$

where F_{OX}^*, F_{OY}^* are the steady, time-averaged forces in a stationary frame and $[A]$ is the rotordynamic matrix where $x(t), y(t)$ are the shaft displacements from the mean position. The steady radial forces F_{OX}^*, F_{OY}^* result from non-axisymmetrics and are discussed in detail elsewhere (Iverson et al [1960], Domm and Hergt [1970], Chamieh [1983], Chamieh et al [1985], Adkins [1985]). We focus here on the rotordynamic

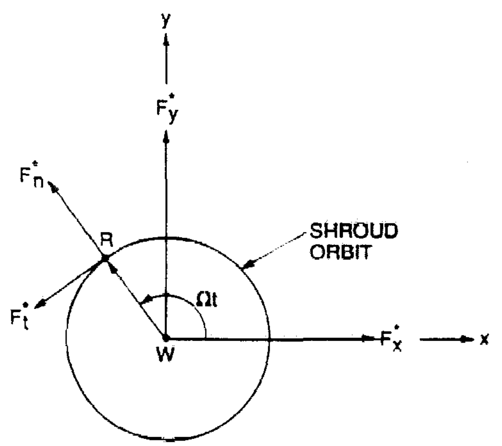

Figure 1. Schematic of the fluid- induced radial forces acting on an impeller whirling in a circular orbit. F_x^* and F_y^* represent the instantaneous forces in the stationary laboratory frame. F_n^* and F_t^* are the forces normal and tangential to the whirl orbit where Ω is the whirl frequency.

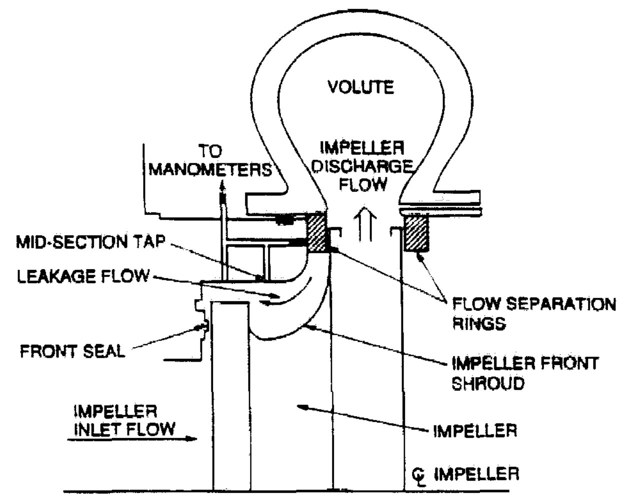

Figure 2. Schematic showing the impeller/volute arrangement for the experiments of Jery (1986) and Adkins (1985).

matrix $[A]$ which will in general be a function not only of the mean flow conditions and pump geometry but also of the whirl motion. In the case of a circular whirl orbit $x = \epsilon \cos \Omega t, y = \epsilon \sin \Omega t$ where ϵ is the eccentricity and Ω is the whirl frequency. Then $[A]$ is expected to be a function of both ϵ and Ω. At small, linear amplitudes $[A]$ should be independent of ϵ and presented as a function of the whirl ratio Ω/ω where ω is the impeller rotation frequency. Then the forces F_n^* and F_t^* normal and tangential to the whirl orbit (figure 1) are given by

$$\begin{aligned} F_n^* &= \epsilon \left(A_{xx} + A_{yy} \right) / 2 \\ F_t^* &= \epsilon \left(A_{yx} - A_{xy} \right) / 2 \end{aligned} \tag{2}$$

Note that if $[A]$ is to be rotationally invariant, then $A_{xx} = A_{yy} = \epsilon^{-1}F_n^*$ and $A_{yx} = -A_{xy} = \epsilon^{-1}F_t^*$. Virtually all of the experimental results confirm the fact that the matrix [A] is rotationally invariant for the flows discussed in this paper (Jery [1986]).

Typical experimental measurements of the dimensionless normal and tangential forces, F_n and F_t, (F_n^*, F_t^* non-dimensionalized by $\rho\pi\omega^2 b_2 \epsilon R_2^2$ where ρ is the fluid density and b_2, R_2 are respectively the width and radius of the impeller discharge) from the work of Jery (1986) are shown in figure 3. These particular results are for a typical five-bladed centrifugal pump impeller made by Byron-Jackson for a specific speed of 0.57 (referred to as Impeller X) and installed in a well-matched spiral volute in the manner shown in figure 2 (for more detail see Jery [1986] or Adkins and Brennen [1988]).

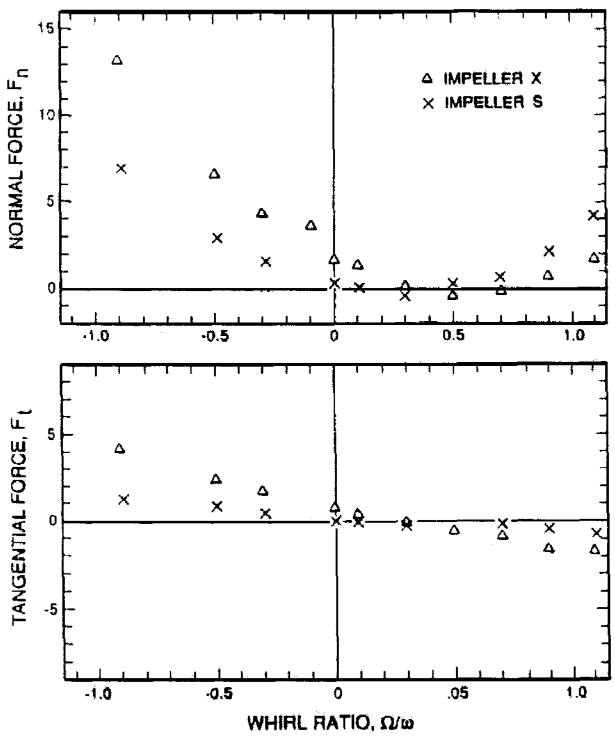

Figure 3. Dimensionless normal and tangential forces, F_n and F_t, as a function of whirl ratio from Jery (1986). Typical centrifugal impeller/ volute combination (Impeller X and Volute A at 1000 rpm and a flow coefficient $\varphi = 0.092$) are shown by Δ; dummy Impeller S results with externally imposed pressure rise are shown by $\times$.

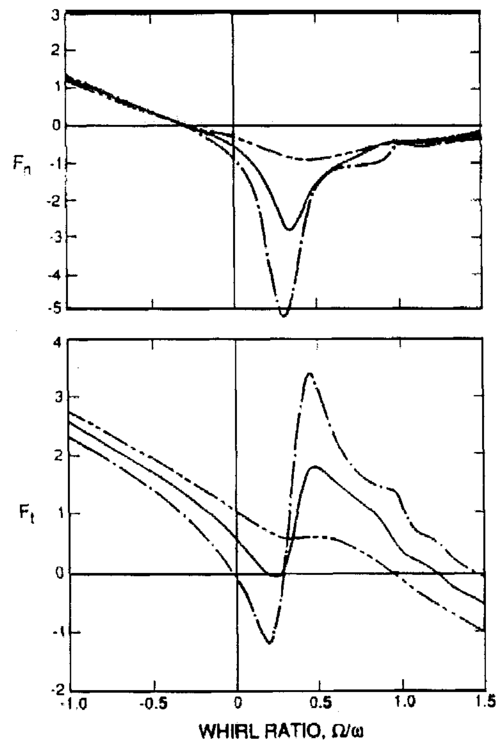

Figure 5. Theoretical predictions from Childs (1986) on the F_n, F_t resulting from the conventional leakage path geometry used in the tests of Bolleter et al (1985). Results are shown for three different inlet swirl velocity conditions in which that swirl velocity is assumed to be 0.5 (— ·· —), 0.6 (——) and 0.7 (— · —) of the shroud inlet rotating velocity.

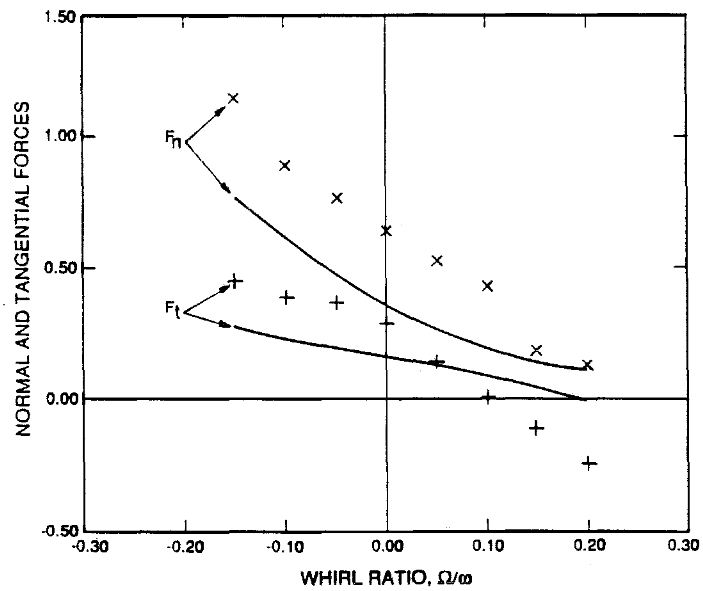

Figure 4. Comparison of the dimensionless normal and tangential forces according to Adkins (1985) theory (solid lines) with the experimental values for Impeller X at $\varphi = 0.092$.

One of the most significant features of these results is the range of positive whirl ratios within which the tangential force is positive and therefore potentially destabilizing rotordynamically. The data for other flow coefficients, φ, is very similar. As these results were being obtained it was recognized that contributions to the rotordynamic forces could arise not only from azimuthally non-uniform pressures in the discharge flow acting on the impeller discharge area but also from similar non-uniform pressures acting on the exterior of the impeller front shroud as a result of the leakage flow passing between this shroud and the pump casing. Consequently, Jery (1986) also made measurements using a solid "impeller" (Impeller S) with the same exterior profile as Impeller X. The leakage flow was simulated by a remote auxiliary pump which generated the same discharge to inlet pressure differences as occurred with Impeller X operating at a given flow coefficient. The normal and tangential forces obtained are included in figure 3. If one assumes that the solid impeller experiences the same leakage flow contributions to F_n, F_t as Impeller X but does not experience the main throughflow contributions, the tentative conclusion could be drawn that the leakage flow contribution to the normal force was about 70% of the total and the contribution to the tangential force was about 30% of the total. This tentative conclusion indicating the substantial role of the leakage flow motivated further study.

In parallel work Adkins (1985) (see also Adkins and Brennen [1988]) developed a fluid mechanical model of the complicated unsteady throughflow generated when a rotating impeller whirls. The model allowed evaluation of the pressure perturbations in the impeller discharge which compared well with the experimental measurements of these perturbations. It therefore permitted evaluation of the contribution to the rotordynamic forces from these pressure perturbations and typical results for a limited range of whirl ratios are presented in figure 4 along with experimental measurements of the total F_n, F_t under the same conditions. The conclusions are crudely consistent with the early remarks; the pressures in the main discharge flow contribute about one half of the rotordynamic forces. To confirm this Adkins (1985) made pressure perturbation measurements in both the main discharge and the leakage flow. These allowed evaluation of the rotordynamic "stiffness," namely the rotordynamic forces at zero whirl ratio, $F_n(0)$ and $F_t(0)$. The experiments suggested fractional contributions similar to those in Jery's work, namely that the leakage flow component of $F_n(0)$ was more than 70% while the component of $F_t(0)$ was about 40%. Adkins (1985) also concluded that changes in the geometry of the leakage pathway resulted in significant changes in these rotordynamic contributions. Since the geometry used in these tests was not typical of that in prototype pumps it was also concluded that further work on the rotordynamic characteristics of leakage flows was clearly indicated and this led to the fabrication of the experiment described below.

There are several other indications which suggest the importance of leakage flows to the fluid-induced rotordynamic forces. It is striking that the total rotordynamic forces measured by Bolleter et al (1987) for a conventional centrifugal pump configuration are about twice the magnitude of those measured by Jery (1986) or Adkins (1985). In the light of the results presented below it now seems sensible to suggest that this difference is due to the fact that the clearances in the leakage flow annulus are substantially smaller in Bolleter's configuration. We also note that there have been reports that SSME impellers fitted with anti-swirl vanes in the leakage flow annulus have had noticeably different rotordynamic charactersitics (Jackson [1985]).

When it became apparent that leakage flows could contribute significantly to the rotordynamics of a pump, Childs (1986) adapted the bulk-flow model which he had developed for the analysis of fluid-induced forces in seals to evaluate the rotordynamic forces, F_n and F_t, due to these leakage flows. The model was applied to several pump geometries; typical results for the conventional centrifugal pump configuration tested by Bolleter et al (1987) are shown in figure 5. The results have been scaled to conform with the non-dimensionalization used in this paper. Data is shown for three different inlet swirl velocity conditions in which the swirl velocity is assumed to be 0.5, 0.6 or 0.7 of the impeller tip speed. Note that Childs (1986) also presents qualitatively similar results for a quite different leakage flow path geometry.

Several general conclusions may be drawn from Childs work. First the magnitude and overall form of the model predictions are consistent with the experimental data. In particular, the model also predicts positive, rotordynamically destabilizing tangential forces (or cross-coupled stiffness to use rotordynamic parlance) over a range of positive whirl ratios. Secondly, a rather unexpected resonance-like phenomenon develops at small positive whirl ratios when the inlet swirl velocity ratio exceeds about 0.5. It remains to be seen whether such "resonances" occur in practice. Childs (1986) points out that a typical swirl velocity ratio at inlet (pump discharge) would be about 0.5 and may not therefore be large enough for the resonance to be manifest. It is clear that a detailed comparison of model predictions with experimental measurement remains to be made and is one of the purposes of the present program.

3. LEAKAGE FLOW TEST APPARATUS

The experimental apparatus sketched in figures 6 and 7 was designed and constructed to simulate impeller shroud leakage flow (Zhuang [1989], Guinzburg et al

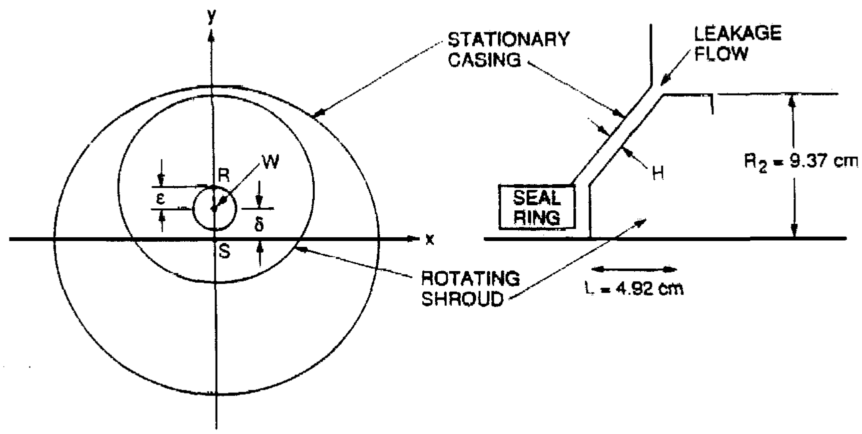

Figure 6. Schematic of the whirling shroud where S is the center of the stationary casing, R is the center of the rotating shroud, W is the center of the whirl orbit along which R travels, $WR = \epsilon$ is the eccentricity, and $WS = \delta$ is the offset.

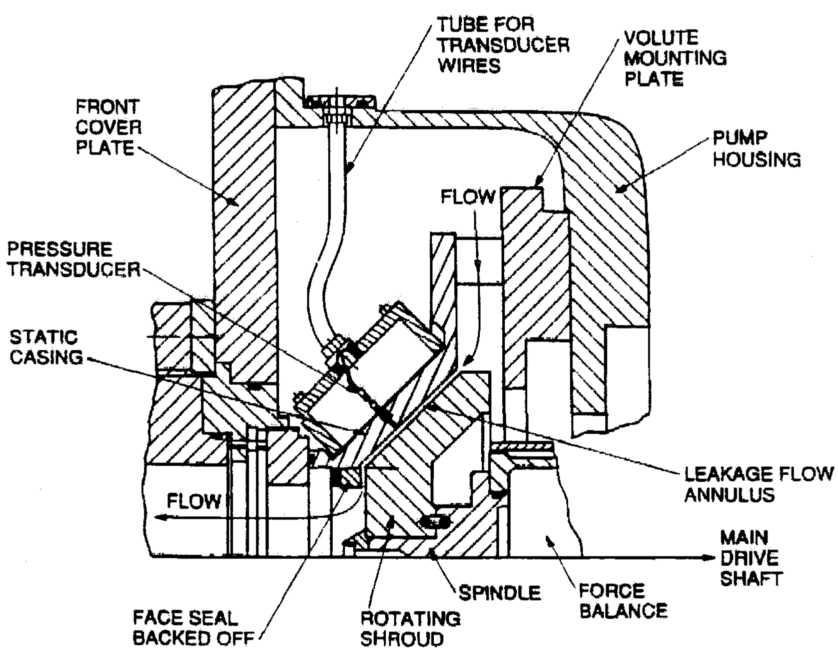

Figure 7. More detailed structure of the leakage flow test apparatus (Zhuang [1989]).

[1990]). A rotating shroud is mounted on a spindle attached to the rotating force balance (Jery et al [1985], Franz et al [1989]). The gap between this rotating shroud and the stationary casing can be varied by both axial and radial adjustment of the stationary casing. The initial geometric configuration consists of a straight annular gap inclined at an angle of 45° to the axis of rotation. The flow through the leakage path is generated by an auxiliary pump. The shroud can be driven at speeds up to 3500 RPM. A circular whirl motion with a frequency up to 1800 RPM can be superimposed on the basic rotation. The amplitude of this whirl motion or eccentricity, ϵ, is variable as is the fixed offset, δ. Both the main motor and the whirl motor are driven through position and velocity feedback systems which are coupled to a data acquisition system which records the position in both rotation cycles at which radial force measurements are taken. Descriptions of the force balance, data processing and other details are contained in Jery (1985).

Steady radial forces and rotordynamic forces were obtained from the force balance measurements. In addition, an array of static pressure manometer taps was located along a meridian in the leakage flow passage. By setting the rotating shroud at various offsets this allowed evaluation of the steady forces and zero whirl frequency rotordynamic forces by integration of the measured pressure differences. These could be compared with the force balance measurements from the same experiments (Zhuang [1989]).

The results from these experiments will be presented non-dimensionally by dividing the forces by $\rho\pi\omega^2 L\epsilon R_2^2$. This differs from the factor used to non-dimensionalize the impeller forces presented earlier in that the axial length, L, of the leakage flow passage (figure 6) has replaced b_2, the impeller discharge width. In most pumps L and b_2 are comparable and hence, to evaluate the significance of the results, the dimensionless data from the leakage flow tests may be directly compared with that from the impeller tests.

The forces are presented as functions of the whirl ratio or ratio of whirl frequency, Ω to rotating frequency, ω. Other dimensionless parameters are the flow coefficient, φ ($= Q/2\pi R_2^2 H\omega$ where Q is the leakage flow rate), the gap width ratio, H/R_2, the eccentricity ratio, ϵ/R_2, the offset ratio, δ/R_2, and the Reynolds number $\omega R_2^2/\nu$, where ν is the kinematic viscosity of the liquid.

4. EXPERIMENTAL RESULTS FOR ROTORDYNAMIC FORCES

Preliminary results from this experimental apparatus were obtained for zero whirl frequency using static offsets (Zhuang [1989]). Typical results for zero flow rate and a particular offset are presented in figure 8 which illustrates a number of general features in the data. Note first that the data at rotating speeds of 1000 rpm and 1500 rpm are in good agreement which provides some evidence that the Reynolds number effects are not too significant. Secondly the forces calculated from the measured pressure distributions in the leakage annulus agree well with those measured directly with the force balance. This confirms the fact that the forces arise from the pressure variations in the leakage flow and not from the viscous shear stresses or the stresses on the other surfaces of the rotating shroud. Finally, figure 8 clearly demonstrates that the forces are a strong function of the clearance, H; indeed the dependence is close to inverse proportionality.

More complete rotordynamic results from force balance measurements are shown in figures 9, 10 and 11 for a rotating speed of 1000 rpm, four different leakage flow rates (zero to 30 gpm), two different clearances, H, and two eccentricities, ϵ. All of the data obtained thus far is for inlet swirl velocity ratios (in Childs' sense) which are close to zero though future tests will explore the effect of this parameter by installation of inlet guide vanes.

Note first that the general form and magnitude of the data shown in figures 9, 10 and 11 is very similar to that obtained for impellers by Jery (1986) and Adkins (1985) and to that from Childs' model in the absence of the "resonance." Secondly,

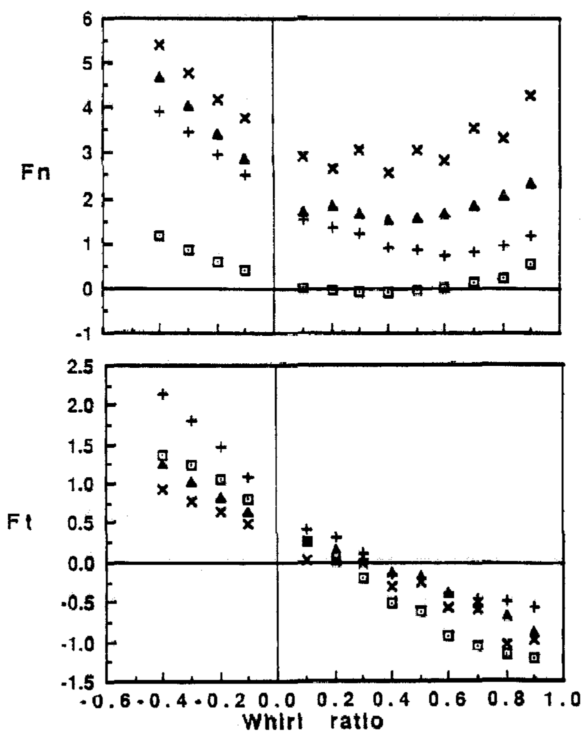

Figure 9. Dimensionless normal and tangential forces at 1000 rpm, an eccentricity $\epsilon = 0.0254$ cm, a clearance, $H = 0.140$ cm, offset, $\delta = 0$ and various flow rates as follows: 0 ℓ/sec = $\square$, 0.631 ℓ/sec (10 gpm) = +, 1.262 ℓ/sec (20 gpm) = Δ, 1.892 ℓ/sec (30 gpm) = $\times$.

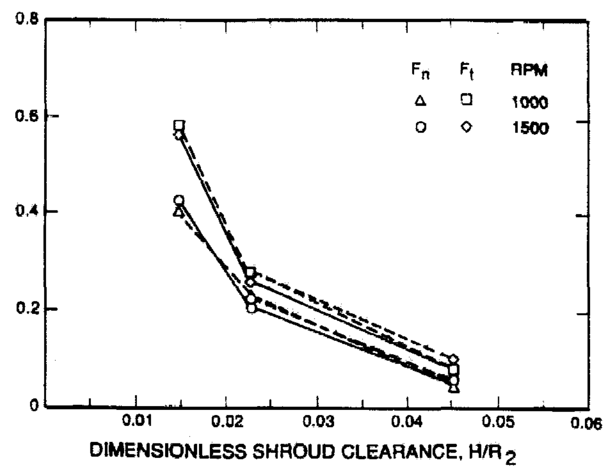

Figure 8. Dimensionless normal and tangential forces at zero whirl frequency, $F_n(0)$ and $F_t(0)$, as a function of the dimensionless shroud clearance, H/R_2 for an eccentricity $\epsilon = 0.076$ cm, an offset $\delta = 0.051$ cm, zero flow rate and two rotating speeds as indicated. Results obtained from pressure measurements (- - - - -) and direct measurements with the force balance (——) are both shown.

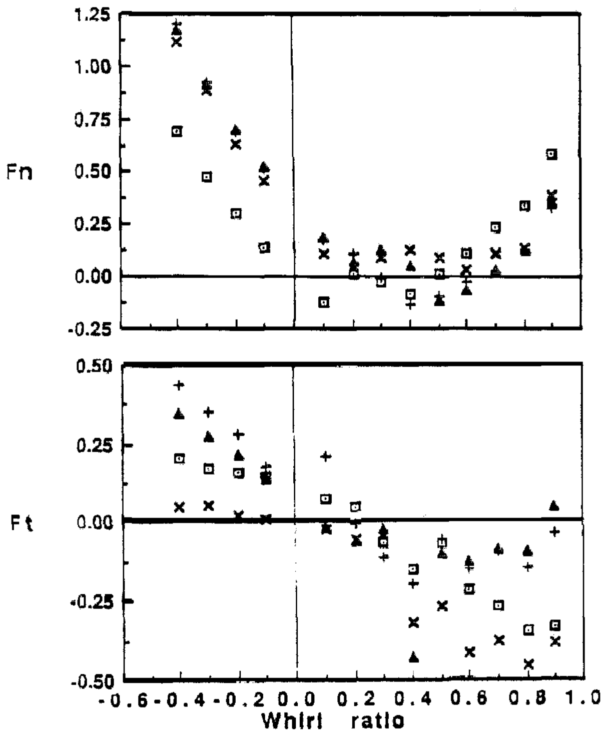

Figure 10. Dimensionless normal and tangential forces at 1000 rpm, an eccentricity $\epsilon = 0.0254$ cm, a clearance $H = 0.424$ cm, offset $\delta = 0$ and various flow rates as follows: 0 ℓ/sec = $\square$, 0.631 ℓ/sec (10 gpm) = +, 1.262 ℓ/sec (20 gpm) = Δ, 1.892 ℓ/sec (30 gpm) = $\times$.

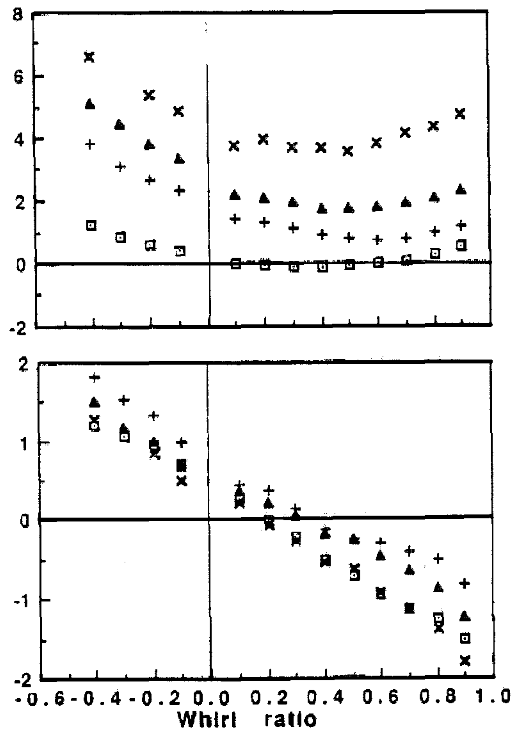

Figure 11. Dimensionless normal and tangential forces at 1000 rpm, an eccentricity $\epsilon = 0.118$ cm, a clearance $H = 0.140$ cm, offset $\delta = 0$ and various flow rates as follows: 0 ℓ/sec = $\square$, 0.631 ℓ/sec (10 gpm) = +, 1.262 ℓ/sec (20 gpm) = Δ, 1.892 ℓ/sec (30 gpm) = $\times$.

since the data of figures 9 and 11 were obtained under conditions which were the same except for the magnitude of the eccentricity, ϵ, it is reassuring to note the similarity between the two sets of data. Evidently these experiments lie within the linear regime of small eccentricities (note that the assumption of linearity was implicit in equation(1)). Thirdly, we note that the forces are strong functions of both the leakage flow rate and the clearance, H. In the case represented by figure 10 the combination of small eccentricity and large clearance led to forces whose magnitudes were rather small and hence the larger scatter in the data presented in that figure.

The effect of flow rate on the normal force is clearer than its effect on the tangential force. Clearly the Bernoulli effect on the normal force increases with increasing flow. It would also appear that the positive tangential forces at small positive whirl ratios are smallest at the highest flow rate and therefore increasing the flow is marginally stabilizing. The effect of the clearance is much larger and it seems that all the forces

TABLE 1

Dimensionless Direct and Cross-coupled Stiffness, Damping and Added Mass from Leakage Flow Tests at 1000 rpm

	Direct Stiffness, K	Cross-Coupled Stiffness, k	Direct Damping, C	Cross-Coupled Damping, c	Direct Added Mass, M
$H = 0.140$ cm, $\epsilon = 0.0254$ cm					
Flow = 0 ℓ/sec	-0.19	0.51	2.18	1.60	2.15
0.631 ℓ/sec	-1.99	0.95	2.10	3.85	3.15
1.262 ℓ/sec	-2.46	0.52	1.55	4.00	4.46
1.892 ℓ/sec	-3.33	0.33	1.49	3.33	4.71
$H = 0.140$ cm, $\epsilon = 0.118$ cm					
Flow = 0 ℓ/sec	-0.17	0.42	2.17	1.64	2.20
0.631 ℓ/sec	-1.81	0.85	1.95	3.59	3.10
1.262 ℓ/sec	-2.77	0.62	1.90	4.20	4.19
1.892 ℓ/sec	-4.36	0.39	2.25	3.79	4.72
$H = 0.424$ cm, $\epsilon = 0.0254$ cm					
Flow = 0 ℓ/sec	-0.048	0.071	0.45	0.91	1.66
0.631 ℓ/sec	-0.299	0.167	0.43	1.60	1.75
1.262 ℓ/sec	-0.330	0.093	0.32	1.50	1.61
1.892 ℓ/sec	-0.312	-0.053	0.43	1.35	1.55

are roughly inversely proportional to the clearance, H.

Though the functional dependence of F_n, F_t on the whirl ratio, Ω/ω, is not necessarily quadratic, it is nevertheless of value to the rotordynamicists to fit the data of figures 9, 10 and 11 to the following expressions:

$$\begin{aligned} F_n &= M\,(\Omega/\omega)^2 - c\,(\Omega/\omega) - K \\ F_t &= -C\,(\Omega/\omega) + k \end{aligned} \tag{3}$$

where M, C, c, K and k are the dimensionless direct added mass (M), direct damping (C), cross-coupled damping (c), direct stiffness (K) and cross-coupled stiffness (k). The cross-coupled added mass (m) has been omitted for simplicity. Table 1 lists the values of these rotordynamic quantities for the data of figures 9, 10 and 11.

The added masses listed in Table 1 could be compared with theoretical values derived as follows. The potential flow added mass for a fluid-filled annulus between two circular cylinders (inner and outer radii denoted by a, b respectively) is $\rho\pi\Delta L a^2 b^2/(b^2 - a^2)$ where ΔL is the axial length (Brennen [1976]); this assumes no axial velocities which could relieve the pressures caused by acceleration of the inner cylinder. If this expression is integrated over the length of the leakage annulus shown in figure 6 it leads to an added mass given by

$$M = 0.160 R_2/H \tag{4}$$

or 3.53 for $H = 0.424$ cm and 10.71 for $H = 0.140$ cm. The fact that the actual values are about 40% of these may reflect the relief allowed by non-zero axial velocity. It is however interesting to note that the above result correctly models the functional dependence on H exhibited by the experimental data.

The data of Table 1 is presented in graphical form in figure 12 where the dimension-

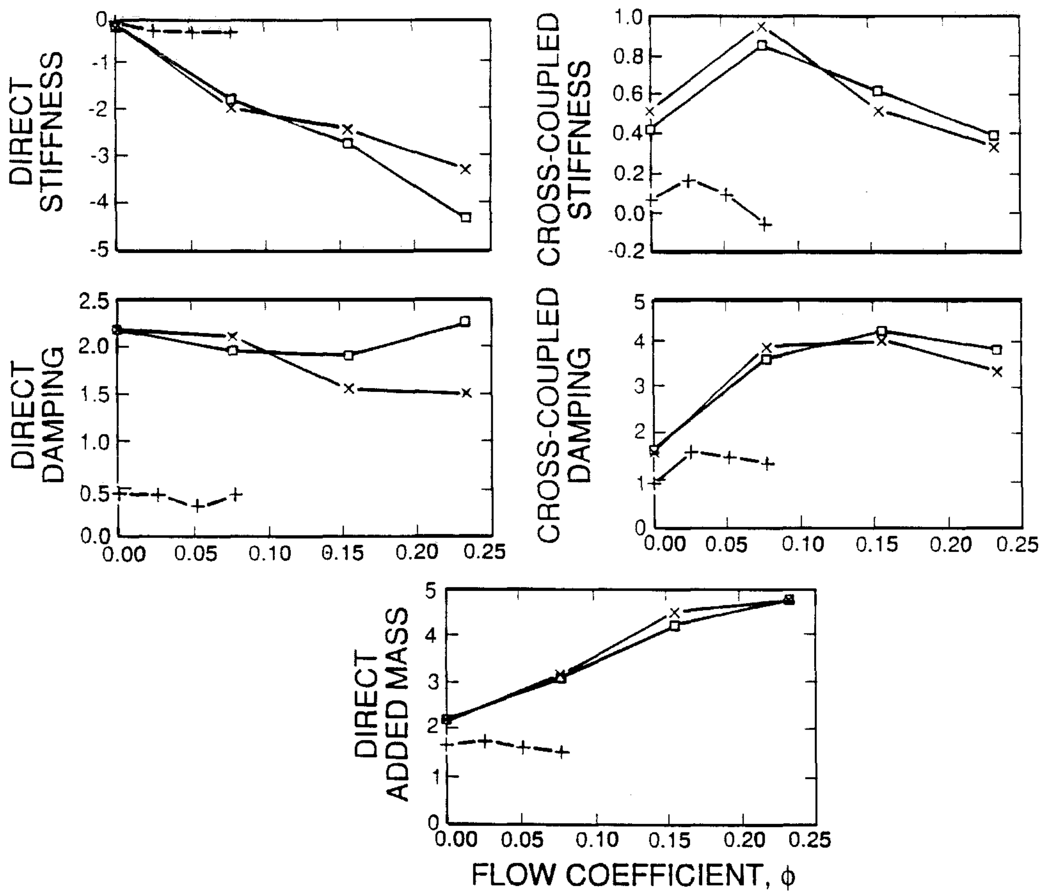

Figure 12. Dimensionless direct and cross-coupled stiffness, damping and added mass as functions of the flow coefficient, φ for three geometries: $\epsilon/R_2 = 0.00271, H/R_2 = 0.0149(\times)$, $\epsilon/R_2 = 0.0126, H/R_2 = 0.0149(\square)$ and $\epsilon/R_2 = 0.00271, H/R_2 = 0.0453(+)$.

less rotordynamic parameters are plotted against the flow coefficient, φ. The similarity of the results for the two eccentricities is clearly manifest. The smaller magnitude generated with the larger clearance is also clearly demonstrated.

5. CONCLUSIONS

A review of the existing experimental and analytical results shows that the discharge-to-suction leakage flow in a centrifugal pump can contribute substantially to the fluid-induced rotordynamic forces for that turbomachine. While the geometry of the impeller shroud/pump casing annulus varies considerably in previous studies the indications are that the contributions from the leakage flow can be of the same order as those acting on the impeller discharge. This motivated the current experimental study of leakage flows and their rotordynamic effects.

Preliminary experimental results for simulated leakage flows of rather simple geometry are presented for different whirl frequencies, eccentricities, clearances and flow rates. The functional dependence on whirl frequency to rotating frequency ratio (termed the whirl ratio) is very similar to that measured in experiments and to that predicted in the theoretical work of Childs. Two sets of results taken at different eccentricities yield quite similar non-dimensional rotordynamic forces indicating that the experiments probably lie within the linear regime. The dimensionless forces are found to be functions not only of the whirl ratio but also of the flow rate and of the clearance. While the dependence on flow rate is not simple, it would appear that the dimensionless rotordynamic forces are roughly inversely proportional to the clearance. Future tests will include the addition of swirl to the inlet flow in order to examine whether the "resonances" predicted by Childs do indeed occur.

6. ACKNOWLEDGEMENTS

The authors are grateful to F. Zhuang, A. Bhattacharyya and F. Rahman for help with the experimental program. We would also like to thank NASA George Marshall Space Flight Center for support under Grant NAG8-118.

7. References:

Adkins, D.E. 1985. Analyses of hydrodynamic forces on centrifugal pump impellers. Ph.D. Thesis, California Institute of Technology, Pasadena, Calif.

Adkins, D.E. and Brennen, C.E. 1988. Analyses of hydrodynamic radial forces on centrifugal pump impellers. ASME J. of Fluids Eng., Vol. 110, No. 1, pp. 20-28.

Bolleter, U., Wyss, A., Welte, I. and Sturchler, R. 1985. Measurements of hydrodynamic interaction matrices of boiler feed pump impellers. ASME Paper No. 85-DET-148.

Brennen, C. 1976. On the flow in an annulus surrounding a whirling cylinder. J. Fluid Mech., Vol. 75, pp. 173-191.

Brennen, C.E., Acosta, A.J. and Caughey, T.K. 1986. Impeller fluid forces. NASA Proc. Advanced Earth-to-Orbit Propulsion Tech. Conf., Huntsville, AL, NASA Conf. Publ. 2436, pp. 270-295.

Chamieh, D.S. 1983. Forces on a whirling centrifugal pump-impeller. Ph.D. Thesis, Division of Eng. and Appl. Sci., California Institute of Technology, Pasadena, Calif.

Chamieh, D.S., Acosta, A.J., Brennen, C.E. and Caughey, T.K. 1985. Experimental measurements of hydrodynamic radial forces and stiffness matrices for a centrifugal pump-impeller. ASME J. of Fluids Eng., Vol. 107, No. 3, pp. 307-315.

Childs, D.W. 1986. Force and moment rotordynamic coefficients for pump-impeller shroud surfaces. Proceedings of Advanced Earth-to-Orbit Propulsion Tech. Conf., Huntsville, AL, May 1986, NASA Conf. Publ. 2436, pp. 296-326.

Domm, U. and Hergt, P. 1970. Radial forces on impeller of volute casing pumps. Flow Research on Blading, editor L.S. Dzung, Elsevier Publ. Co., Netherlands, pp. 305-321.

Franz, R., Acosta, A.J., Brennen, C.E. and Caughey, T.K. 1989. The rotordynamic forces on a centrifugal pump impeller in the presence of cavitation. Proc. of 3rd Joint ASCE/ASME Mechanics Conf., UCSD, July 1989, Pumping Machinery, Vol. 81, pp. 205-212.

Guinzburg, A., Brennen, C.E., Acosta, A.J. and Caughey, T.K. 1990. Measurements of the rotordynamic shroud forces for centrifugal pumps. ASME Turbomachinery Forum, Toronto, Canada, June 1990.

Hergt, P. and Krieger, P. 1969-70. Radial forces in centrifugal pumps with guide vanes. Proc. Inst. Mech. Eng., Vol. 184, Part 3N, pp. 101-107.

Iversen, H.W., Rolling, R.E. and Carlson, J.J. 1960. Volute pressure distribution, radial force on the impeller and volute mixing losses of a radial flow centrifugal pump. ASME J. of Eng. for Power, Vol. 82, No. 2, pp. 136-144.

Jackson, E. 1985. Personal communication.

Jery, B., Acosta, A.J., Brennen, C.E. and Caughey, T.K. 1985. Forces on centrifugal pump impellers. Second International Pump Symposium, Houston, TX, April 29-May 2, 1985.

Jery, B. 1986. Experimental study of unsteady hydrodynamic force matrices on whirling centrifugal pump impellers. Ph.D. Thesis, California Institute of Technology, Pasadena, Calif.

Zhuang, F. 1989. Experimental investigation of the hydrodynamic forces on the shroud of a centrifugal pump impeller. Report No. E249.9, Division of Eng. and Appl. Sci., California Institute of Technology, Pasadena, Calif.